Shape-dependent rheology of dry granular flows studied by LS-DEM

Haoran Jiang, Reid Kawamoto, Takashi Matsushima

▶ **To cite this version:**

Haoran Jiang, Reid Kawamoto, Takashi Matsushima. Shape-dependent rheology of dry granular flows studied by LS-DEM. 13th International Conference on Geotechnique, Construction Materials & Environment, Nov 2023, Mie University, Tsu, Japan. ⟨hal-04763182⟩

HAL Id: hal-04763182

https://hal.science/hal-04763182v1

Submitted on 1 Nov 2024

HAL is a multi-disciplinary open access archive for the deposit and dissemination of scientific research documents, whether they are published or not. The documents may come from teaching and research institutions in France or abroad, or from public or private research centers.

L'archive ouverte pluridisciplinaire **HAL**, est destinée au dépôt et à la diffusion de documents scientifiques de niveau recherche, publiés ou non, émanant des établissements d'enseignement et de recherche français ou étrangers, des laboratoires publics ou privés.

HAL Authorization

13th Int. Conf. on Geotechnique, Construction Materials & Environment, Tsu, Mie, Japan, 14-16 November 2023, ISBN 978-4-909106100 C3051

SHAPE-DEPENDENT RHEOLOGY OF DRY GRANULAR FLOWS STUDIED BY LS-DEM

Haoran Jiang[1], Reid Kawamoto[2] and Takashi Matsushima[1]

[1]Department of Engineering Mechanics and Energy, University of Tsukuba, Tsukuba, Japan
[2] Independent Scholar, Tsukuba, Japan

ABSTRACT

Predicting the behavior of granular flows is of primary importance in preventing geo-disasters. A key to progress is the building of constitutive laws for describing complex granular flows. This paper investigates dry, frictional granular flows consisting of superellipses utilizing the 2D level set discrete element method (LS-DEM). Simple shear tests were performed on dense samples of different shapes under varying shearing speeds, and an empirical rheology model was examined and revised. The sphericity S, a low-order shape parameter, is used to describe the particle shapes in this study, which incorporates two shape features considered in the present study (i.e., elongation α and blockiness n). The study shows that the quasi-static shear strength μ_0 is a decreasing function of S, with an almost linear dependency for the shapes explored. We further proposed a simple dimensionless parameter I_S, which incorporates the sphericity S into the original inertial number I, to describe the dynamic component of shear strength, $\Delta\mu(I_S)$. Surprisingly, it is observed that all curves from the three groups of shapes collapse into a nearly identical curve, indicating the validity of I_S. These results contribute to the establishment of a more universal $\mu(I)$ rheology model for complex granular systems.

Keywords: LS-DEM, Granular flow, Shape effect, Rheology model

INTRODUCTION

Mechanics of granular materials has experienced rapid development in recent decades stimulated by the insufficiency of existing theories to meet the demands of engineering practice [1, 2]. Particularly, dense granular flows [3, 4] have garnered much attention and made considerable progress owing to their prevalence in everyday life, such as landslides, avalanches, and other geological disasters. Dense granular flows exhibit yield threshold and shear rate dependence [3], which makes them considered to be visco-plastic materials. Consequently, the Herschel-Bulkley type model [5] is applicable to describe their flow properties, such as the widely accepted $\mu(I)$ rheology model [6, 7]. This model introduces the dimensionless inertial number

$$I = \dot{\gamma} d / \sqrt{P/\rho}\,, \tag{1}$$

a rescaled shear rate $\dot{\gamma}$ normalized by the particle size d, the confining pressure P and the particle density ρ, to characterize the behavior of granular flows. It effectively captures the changing dissipative behavior within the granular materials as overall flow state changes. Specifically, as mobility, indicated by I, increases, the dissipative characteristics $\mu = \tau/P$ (τ is the local shear stress) inside the flow strengthen, constraining the growth of mobility and leading to the steady-state flow [8]. The mathematical form is

$$\mu(I) = \mu_0 + \Delta\mu(I) = \tau_0/P + \Delta\mu(I), \tag{2}$$

where τ_0 is the yield stress. The quantity $\Delta\mu$, referred to as the dynamic component of shear strength, displays a monotonically increasing trend as the inertial number I increases, which is commonly fitted by the non-linear expression [7, 9]: $\Delta\mu(I) = \Delta\mu_m/(1 + I_0/I)$, or the power-law scaling [10, 11]: $\Delta\mu(I) = AI^a$. Previous studies have tested the validity of this model in various settings with distinct boundary conditions, such as the gravity-free simple shear cell [8, 12] and the rough inclined plane [9, 13]. The local stress τ is found to be dependent on the local flow properties, such as shear rate $\dot{\gamma}$, making the $\mu(I)$ model a local rheology model.

However, the model has some limitations, as it lacks a connection with the microscopic mechanism of granular flow behavior and is mainly derived from empirical analysis [3]. Furthermore, the rheological properties of granular materials exhibit significant non-local effects [14–16] near the yield threshold in certain complex geometries, such as the simple shear cell with gravity [15, 16]. This can be described by considering the "secondary rheology" that takes into account the effect of the non-local characteristic length [15]. Additionally, the model is based on granular materials consisting of dry monodisperse disks/spheres, whereas in most real granular materials, irregular shapes, cohesive forces, interaction with interstitial fluids, and size polydispersity are frequently encountered. Therefore, describing

granular materials more complex than simple dry monodisperse disks/spheres is another challenge [3]. To address this issue, Vo [17] introduced a modified inertial number I_m that incorporates the impact of capillary, viscous and inertial forces, and successfully predicted the behavior of wet granular flows. Man [18] incorporated the influence of inter-particle friction and established a relation between the newly proposed new dimensionless number M and system rheology. Jiang [9] defined a generalized inertial number $\hat{I}$ by replacing d in Eq. (1) with the proposed characteristic length $\langle d \rangle$, which is determined by the contact ratios of large and small particles in a given bi-disperse system. This methodology leads to the collapsing of the dynamic component $\Delta\mu(\hat{I})$ of all systems onto a single unique curve. These efforts have resulted in the fine-tuning and improvement of the original rheological law, thereby enriching a more comprehensive constitutive framework for complex granular systems.

This paper aims to establish a rheological model that incorporates the particle shape effect, through the analysis of the granular flows comprised of superelliptic particles. The discrete element method (DEM) [19] is utilized in modeling the granular flows, where a sophisticated level-set contact scheme is incorporated, specifically referred to as the level set discrete element method (LS-DEM) [20]. While some previous studies [11, 21, 22] have examined the rheological properties of systems with specific non-circular shapes, there is currently no comprehensive model to describe the rheology of particles with different shapes. This is because a universal shape parameter that can capture diverse shape features, such as elongation, angularity, and non-convexity, has yet to be identified. To overcome this limitation, we propose using sphericity S as a simple, low-order shape parameter to describe particle shape. Based on this parameter, we present a shape-dependent rheology model.

SUPERELLIPSE MODELING

Properties of Superellipse

The surface points (x, y) of a standard superellipse in the Cartesian coordinate system satisfy

$$|x/a|^n + |y/b|^n = 1, \tag{3}$$

where the shape is characterized by the elongation $\alpha = a/b$ and the blockiness n. In this paper, we focus on the convex shapes with $\alpha \in [1, 3]$ and $n \in [2, 50]$. It is worth noting that when $\alpha = 1$ and $n = 2$, the shape is a disk. Moreover, particles with $\alpha > 1$ and $n = 2$ or $\alpha = 1$ and $n > 2$ correspond to the ellipse or superdisk series, respectively. The area of a superellipse can be explicitly given by

$$A_p = (4ab/n)B(1/n\,, 1/n + 1), \tag{4}$$

where $B(x, y)$ represents the beta function. Furthermore, the moment of inertia can be also expressed in terms of the beta function as

$$I_z = [ab(a^2 + b^2)/n]B(3/n\,, 1/n). \tag{5}$$

Level-set Based Contact Algorithm

In the context of LS-DEM, two key ingredients are responsible for the shape representation and contact detection, including: (i) discrete nodes seeded onto the particle surface; and (ii) a uniform grid enclosing the particle, with each grid point storing the corresponding level-set value. The contact is determined by a node-to-surface scheme, which checks the discrete nodes of particle i against the boundary constructed by the level-set grid of particle j (see Fig.1a).

Unlike the clump or polyhedra method, where the number of sub-particles or faces largely changes the underlying geometry, the particle shape in LS-DEM is decided by the level set function mentioned below, irrespective of the density of the surface nodes. A higher node density can lead to improved contact detection sensitivity but increases computational costs (Fig.1b). In this study, 152 surface points seeding on the particle surface are maintained for all simulations, which is sufficiently large to meet the requirement that the node spacing should be no greater than $d/10$ [20].

As for the selection of level set function, the signed distance function (SDF) $\varphi(\boldsymbol{x})$ is adopted in the present study to describe the superelliptic shape.

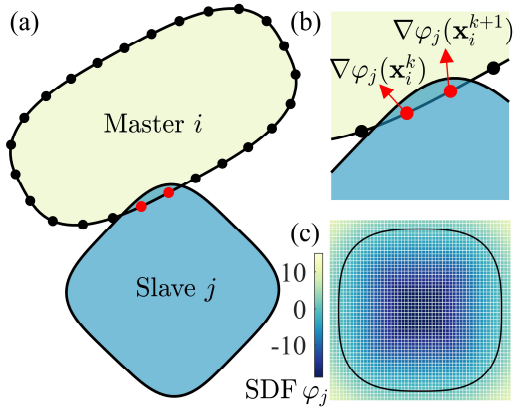

Fig.1 (a) Schematic of the node-to-surface contact scheme and (b) its zoom-in view. The penetration is exaggerated for clarity. (c) Signed distance function (SDF) with the values storing in a grid.

The SDF measures the scalar distance from a point $\boldsymbol{x}$ to the particle interface Ω, with positive or negative sign indicating the particle exterior Ω^+ or interior Ω^- (Fig.1c). One of the advantages of adopting the SDF in this framework is that its value $\varphi(\boldsymbol{x})$ and gradient $\nabla\varphi(\boldsymbol{x})$ stand for the penetration depth and contact normal vector, which are necessary for the regular DEM calculation. For more details about this scheme, the reader is referred to Kawamoto *et al.* [20].

Force Computation and Motion

Given the contact information of particle pairs, the force and moment on the particle can be calculated in terms of a simple spring-damping model with a slider [19]. The normal and tangential forces are calculated from the penetration depth and relative velocity of two particles. Furthermore, the Coulomb friction law is applied to account for slip motion when the magnitude of tangential force exceeds the threshold decided by inter-particle friction μ_p and normal force. The frictional force computed in this way is history-dependent and should be stored for the next time step. Finally, the translational velocity, angular speed, position, and rotation of the particle are updated using forward Euler integration with an appropriate time step Δt.

NUMERICAL SIMULATIONS

The numerical simulations were carried out using the above-mentioned LS-DEM approach. Three different shape groups were investigated: (G1) ellipses ($n = 2$) with varying elongations ($\alpha \in \{1, 1.1, 1.2, 1.3, 1.4, 1.5, 2, 3\}$), (G2) superdisks ($\alpha = 1$) with varying blockiness ($n \in \{2, 2.4, 3, 3.4, 4, 5, 10, 50\}$), and (G3) general superellipses with both shape features, where shapes are determined by the combinations of $\alpha \in \{1.2, 1.4, 2\}$ and $n \in \{3, 4, 50\}$. A total of 24 samples of different shapes were obtained, where each sample consisted of $n_p = 10000$ particles generated randomly within a double periodic domain. The effective diameters d', defined as the diameters of disks with the same areas as the particles, were distributed uniformly between 0.67 and 1.33, with a mean $\overline{d'} = 1$. The samples were then slowly compressed by changing the periodic length in two dimensions. The compression continued until: (i) the system stresses $\sigma_{xx} = \sigma_{yy}$ reached the target confined pressure $P = 100$; (ii) the system energy fell below a small value $E_k < 10^{-6}$. Note that the gravity and inter-particle friction μ_p were turned off to obtain dense samples with mechanical uniformity. Figure 2 depicts zoom-in views of the circular, G1, G2, and G3 samples at the end of isotropic compression. The obtained dense samples were then subjected to simple shear by applying the opposite lateral speeds to the rigid walls obtained by fixing the particles near the upper and lower boundaries. Additionally, along the vertical direction, the bottom wall was fixed, and the top wall was allowed to move to maintain the system stress $\sigma_{yy} = P$. During the shear, the inter-particle friction μ_p was reset to 0.5, corresponding to the surface friction of most natural granular materials. The present study aims to investigate the behavior of dense flows characterized by the inertial number, with I varying in the range of 10^{-3} to 0.25. The LS-DEM simulation parameters are summarized and presented in Table 1.

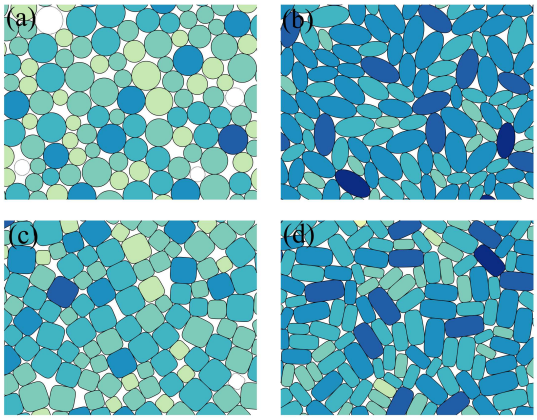

Fig.2 Samples obtained from isotropic compression tests: (a) $\alpha = 1$, $n = 2$ (disk), (b) $\alpha = 2$, $n = 2$ (G1), (c) $\alpha = 1$, $n = 4$ (G2), and (d) $\alpha = 2$, $n = 4$ (G3). Color intensity indicates the contact number, and dashed lines indicate the rattlers.

Table 1 LS-DEM simulation parameters

Parameter	Notation	Value
Number of particles	n_p	10000
Particle size and dispersity	$\langle d \rangle \pm \epsilon$	1 ± 0.33
Coefficient of restitution	e	0.1
Inter-particle friction	μ_p	0 (compression)
		0.5 (shear)
Normal stiffness	k_n	$400P$
Shear stiffness	k_s	$1.0k_n$
Simulation time step	Δt	$10^{-5}s$

MACROSCOPIC BEHAVIOR

Figure 3 shows the snapshots of samples under quasi-static shear in the critical state. The force networks are represented by the segments connecting the particle centers and contact points, where the thickness is proportional to the force

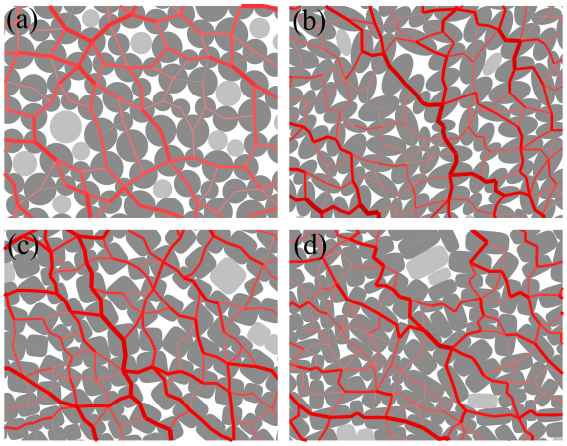

Fig.3 Samples subjected to simple shear at the critical state: (a) $\alpha = 1$, $n = 2$ (disk), (b) $\alpha = 2$, $n = 2$ (G1), (c) $\alpha = 1$, $n = 4$ (G2), and (d) $\alpha = 2$, $n = 4$ (G3), together with force network. Line thickness is proportional to the magnitude of normal forces.

magnitude. Note that shear strength μ is evaluated from the steady state (or critical state) by analyzing the system stress tensors $\sigma_{\alpha\beta} = (\sum_{i<j} f_\alpha^{ij} l_\beta^{ij})/A$, where f_α^{ij}, l_β^{ij} are the $\alpha-$component of the contact force, $\beta-$component of the branch vector, and A represents the system area. Figure 4 displays the dependence of shear strength μ on the original inertial number I for all three different shape groups. The results obtained for the circular system are found to be consistent with previous studies using regular DEM simulations (Fig.4a), indicating the reliability of our LS-DEM simulations. For non-circular systems, the shear strength μ also increases with inertial number, but the quasi-static strength μ_0 and dynamic component $\Delta\mu(I)$ vary significantly across different shapes. Note that the difference in μ_0 is purely due to the varying shape while independent of the way to define the inertial number. Previous studies have shown that the hindrance to particle rotations is the primary contributor to the shear resistance of non-circular shapes. Therefore, it is crucial to find a parameter that can reflect this effect. In our study, sphericity S, the radii ratio of the maximum inscribed disk to the minimum circumscribed disk, is used as a candidate for this purpose. Figure 5 presents the definition of sphericity and the values of this parameter for all shapes explored in this study. Despite being a low-order parameter, sphericity incorporates various shape features, including the elongation α and blockiness n considered in the present study. Figure 6 shows the quasi-static strength μ_0 of all three groups of systems as a function of sphericity S. As anticipated, a lower S

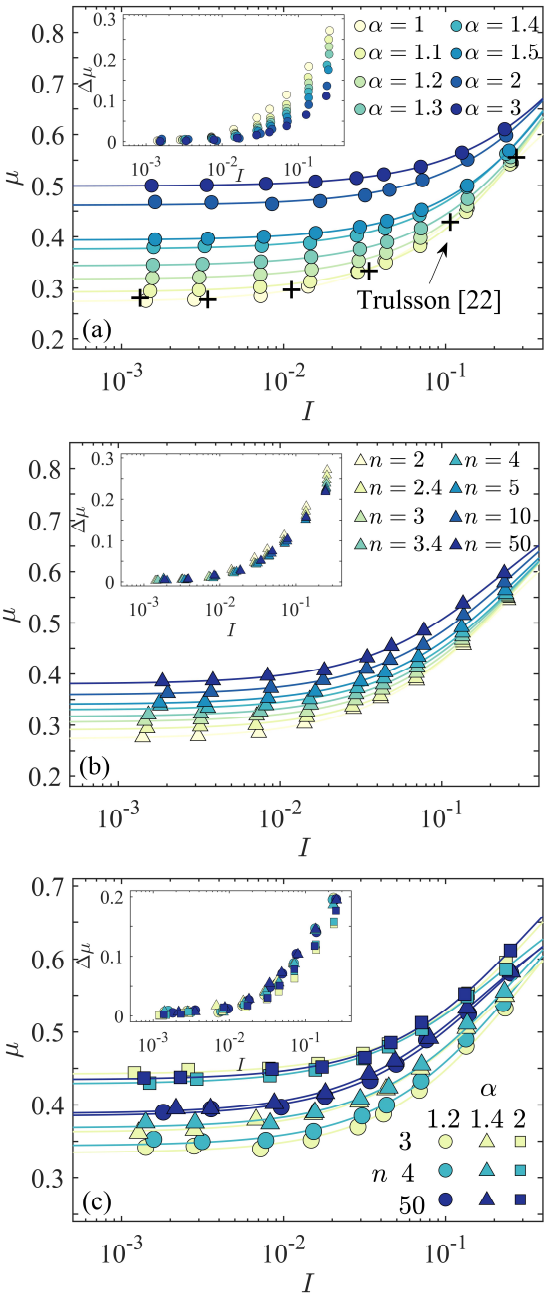

Fig.4 Shear strength μ as a function of original inertial number I in log-linear scale, along with best fits using the non-linear expression. Inset: $\Delta\mu = \mu - \mu_0$ as a function of I.

contributes to a higher μ_0. More surprisingly, an almost linear relationship between the two parameters can be observed, despite small variations across different shape groups. Moreover, data from previous literature on two additional non-circular shapes, namely the rounded-cap rectangle (RCR) and trimer, are extracted and included in our analysis [23, 24]. Figure 6 illustrates examples of these two shapes and the corresponding data points. Interestingly, these data

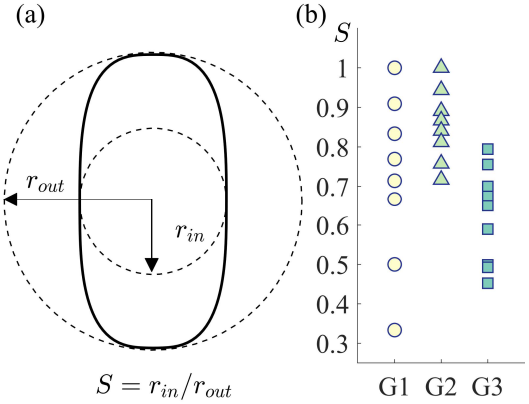

Fig.5 (a) Definition of the sphericity S, and (b) values of S for explored shapes.

points are consistent with those for our superellipse systems. This suggests that sphericity S may be useful in predicting the quasi-static response of shapes belonging to rounded family (i.e., particles with gradually deviating shapes from a disk).

Another focus is the dynamic component of shear strength $\Delta\mu$ resulting from the increase in flow speed, which is attributed to the higher energy dissipation. Although the quasi-static shear strength μ_0 varies with shape, our observations indicate that all $\mu(I)$ curves of different shapes intersect eventually, provided the inertial number I is sufficiently large. This suggests a gradual weakening and eventual vanishing of the shape effect. It is due to in the dilute regime (when I is large enough), particle interactions are dominated by instantaneous binary collisions and the rotation hindrance caused by the shape is not as effective as in dense conditions. And this leads to the observed variations in the $\Delta\mu(I)$ curves as the shape varies (see insets in Fig.4). In view of this, we propose a new dimensionless parameter $I_S = SI$ to replace the original inertial number, which incorporates the

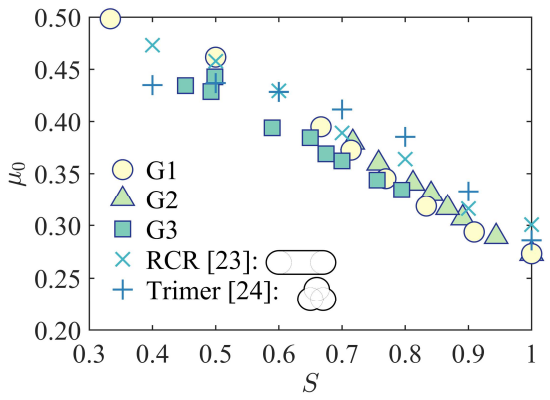

Fig.6 Quasi-static shear strength μ_0 as a function of sphericity S. Data of two other shape groups are extracted from Refs. [23, 24].

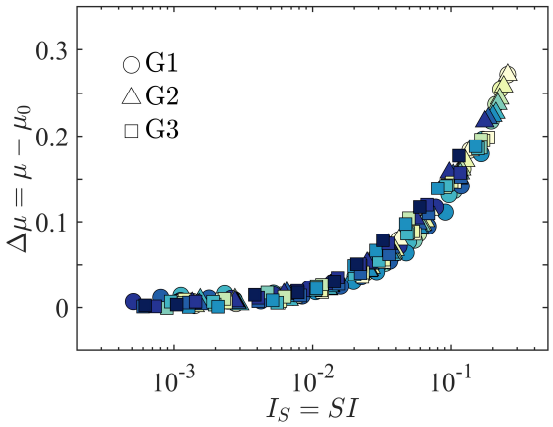

Fig.7 Dynamic component of shear strength $\Delta\mu$ as a function of the shape-dependent inertial number I_S from three shape groups.

effect of sphericity. Remarkably, $\Delta\mu(I_S)$ obtained from all the shapes we consider in our study fall almost on an identical curve, highlighting the generality of this sphericity-based rheology model, even though the physical interpretation involved remains uncertain. As discussed previously, the quasi-static limit μ_0 can be also modeled as a linear function of sphericity, which enables us to predict the shear strength μ of any superellipse system at any shear speed with the help of sphericity. It is worth noting that our study only focuses on frictional systems, and further study is needed to investigate whether our findings remain valid for frictionless systems, where the slip motion of particles is more prevalent.

CONCLUSIONS

To conclude, this study employs the two-dimensional level set discrete element method (LS-DEM) to explore the shape effect on the shear strength of granular flows consisting of superellipses. A total of 24 dense samples were prepared by isotropic compression tests and subjected to simple shear at varying shearing speeds, giving altogether 216 granular systems being systematically analyzed. We find the following. (i) The quasi-static shear strength μ_0 can be described as a nearly linear function of particle sphericity S. Specifically, lower S was found to correspond to higher μ_0 and thus, the circles exhibit the lowest shear resistance. (ii) A shape-dependent, new dimensionless parameter I_S was proposed and proved to be efficient to unify the dynamic component of shear strength $\Delta\mu(I_S)$ of all explored shapes. Note the shapes considered in this study encompasses a wide range of the superellipses, thereby highlighting the generalizability of these results within a broader range of the superellipse family. However, the findings we have observed lack

a clear understanding of the microscopic mechanisms behind them. Therefore, it is essential to conduct further research to develop a fundamental theory that can explain these results. Given that the present study is based on the frictional particles, it is necessary to validate the findings in frictionless granular systems that promote slip motion. Moreover, establishing a unified rheology framework capable of addressing more complex shapes remains a significant challenge in the field.

ACKNOWLEDGMENTS

H.J. acknowledges the financial support of JST-SPRING program, Grant Number JPMJSP2124.

REFERENCES

[1] Gray, J.M.N.T., Particle segregation in dense granular flows. Annual Review of Fluid Mechanics, 50, 2018, pp.407-433.

[2] Yu, F., Particle breakage in granular soils: a review. Particulate Science and Technology, 39(1), 2021, pp.91-100.

[3] Forterre, Y. and Pouliquen, O., Flows of dense granular media. Annu. Rev. Fluid Mech., 40, 2008, pp.1-24.

[4] Pellegrino, A.M. and Schippa, L., Macro viscous regime of natural dense granular mixtures. GEOMATE Journal, 4(7), 2013, pp.482-489.

[5] Herschel, W.H. and Bulkley, R., Konsistenzmessungen von gummi-benzollösungen. Kolloid-Zeitschrift, 39, 1926, pp.291-300. (in German)

[6] GDR MiDi, On dense granular flows. The European Physical Journal E, 14, 2004, pp.341-365.

[7] Jop, P., Forterre, Y. and Pouliquen, O., A constitutive law for dense granular flows. Nature, 441(7094), 2006, pp.727-730.

[8] Da Cruz, F., Emam, S., Prochnow, M., Roux, J.N. and Chevoir, F., 2005. Rheophysics of dense granular materials: Discrete simulation of plane shear flows. Physical Review E, 72(2), p.021309.

[9] Jiang, H., Jiang, X. and Matsushima, T., Rheology of segregated bi-disperse flow in an inclined plane. Journal of JSCE, 11(2), 2023, pp.22-15035.

[10] Hatano, T., Power-law friction in closely packed granular materials. Physical Review E, 75(6), 2007, p.060301.

[11] Azéma, É., Radjaï, F. and Roux, J.N., Inertial shear flow of assemblies of frictionless polygons: Rheology and microstructure. The European Physical Journal E, 41, 2018, pp.1-12.

[12] Liu, D. and Henann, D.L., Size-dependence of the flow threshold in dense granular materials. Soft matter, 14(25), 2018, pp.5294-5305.

[13] Rognon, P.G., Roux, J.N., Naaïm, M. and Chevoir, F., Dense flows of bidisperse assemblies of disks down an inclined plane. Physics of Fluids, 19(5), 2007, p.058101.

[14] Koval, G., Roux, J.N., Corfdir, A. and Chevoir, F., Annular shear of cohesionless granular materials: From the inertial to quasistatic regime. Physical Review E, 79(2), 2009, p.021306.

[15] Kamrin, K. and Koval, G., Nonlocal constitutive relation for steady granular flow. Physical review letters, 108(17), 2012, p.178301.

[16] Robinson, J.A., Holland, D.J. and Fullard, L., Granular packing in complex flow geometries. Physical Review Fluids, 7(7), 2022, p.074304.

[17] Vo, T.T., Nezamabadi, S., Mutabaruka, P., Delenne, J.Y. and Radjai, F., Additive rheology of complex granular flows. Nature communications, 11(1), 2020, p.1476.

[18] Man, T., Zhang, P., Ge, Z., Galindo-Torres, S.A. and Hill, K.M., Friction-dependent rheology of dry granular systems. Acta Mechanica Sinica, 39(1), 2023, p.722191.

[19] Cundall, P.A. and Strack, O.D., A discrete numerical model for granular assemblies. geotechnique, 29(1), 1979, pp.47-65.

[20] Kawamoto, R., Andò, E., Viggiani, G. and Andrade, J.E., Level set discrete element method for three-dimensional computations with triaxial case study. Journal of the Mechanics and Physics of Solids, 91, 2016, pp.1-13.

[21] Jiang, X. and Matsushima, T., Rheological and Microstructural Characteristics in Granular Shear Flow of 2d Elliptical Particles. Journal of Japan Society of Civil Engineers, Ser. A2 (Applied Mechanics (AM)), 77(2), 2021, pp.I_297-I_305.

[22] Trulsson, M., Rheology and shear jamming of frictional ellipses. Journal of Fluid Mechanics, 849, 2018, pp.718-740.

[23] Azéma, E. and Radjaï, F., Stress-strain behavior and geometrical properties of packings of elongated particles. Physical Review E, 81(5), 2010, p.051304.

[24] Saint-Cyr, B., Voivret, C., Delenne, J.Y., Radjai, F. and Sornay, P., Effect of shape nonconvexity on the shear strength of granular media. In AIP Conference Proceedings, Vol. 1145, No. 1, 2009, pp. 389-39